

Radiative $\Omega_Q^* \rightarrow \Omega_Q \gamma$ and $\Xi_Q^* \rightarrow \Xi'_Q \gamma$ transitions in light cone QCD

T. M. Aliev^{*†}, K. Azizi[‡], H. Sundu[§]

[†] Department of Physics, Middle East Technical University, 06531, Ankara, Turkey

[‡] Department of Physics, Doğuş University, Acıbadem-Kadıköy, 34722 Istanbul, Turkey

[§] Department of Physics, Kocaeli University, 41380 Izmit, Turkey

Abstract

We calculate the magnetic dipole and electric quadrupole moments associated with the radiative $\Omega_Q^* \rightarrow \Omega_Q \gamma$ and $\Xi_Q^* \rightarrow \Xi'_Q \gamma$ transitions with $Q = b$ or c in the framework of light cone QCD sum rules. It is found that the corresponding quadrupole moments are negligibly small while the magnetic dipole moments are considerably large. A comparison of the results on the considered multipole moments as well as corresponding decay widths with the predictions of the vector dominance model is performed.

PACS: 11.55.Hx, 13.40.Em, 13.40.Gp, 13.30.Ce, 14.20.Lq, 14.20.Mr

*Permanent address: Institute of Physics, Baku, Azerbaijan

[†]e-mail: taliev@metu.edu.tr

[‡]e-mail: kazizi@dogus.edu.tr, kazem.azizi@cern.ch

[§]e-mail: hayriye.sundu@kocaeli.edu.tr

1 Introduction

In the recent years, there have been significant experimental progresses on hadron spectroscopy. Many new baryons containing heavy bottom and charm quarks as well as many new charmonium like states are observed. Now, all heavy baryons with single heavy quark have been discovered in the experiments except the Ω_b^* baryon with spin-3/2. In the case of doubly heavy baryons only the doubly charmed Ξ_{cc} baryon has been discovered by SELEX Collaboration [1, 2] but the experimental attempts on the identification of other members of the doubly baryons as well as triply heavy baryons predicted by quark model are continued. Considering these progresses and facilities of experiments specially at LHC, it would be possible to study the decay properties of heavy baryons in near future. Theoretical studies on electromagnetic, weak and strong decays of heavy baryons receive special attention in the light of the experimental results.

In the present work we calculate the electromagnetic form factors of the radiative $\Omega_Q^* \rightarrow \Omega_Q \gamma$ and $\Xi_Q^* \rightarrow \Xi_Q' \gamma$ transitions in the framework of the light cone QCD sum rules as one of the most applicable non-perturbative tools to hadron physics. Here, baryons with * correspond spin-3/2 while those without * are spin-1/2 baryons. Using the electromagnetic form factors at static limit ($q^2 = 0$), we obtain the magnetic dipole and electric quadrupole moments as well as decay widths of the considered radiative decays. We compare our results with the predictions of the vector meson dominance model (VDM) [3] which uses the values of the strong coupling constants between spin-3/2 and spin-1/2 heavy baryons with vector mesons [4] to calculate the magnetic dipole and electric quadrupole moments of the transitions under consideration. The electromagnetic multipole moments of heavy baryons can give valuable information on their internal structure as well as their geometric shapes. Note that other possible radiative transitions among heavy spin-3/2 and spin-1/2 baryons with single heavy quark, namely $\Sigma_Q^* \rightarrow \Sigma_Q \gamma$, $\Xi_Q^* \rightarrow \Xi_Q \gamma$ and $\Sigma_Q^* \rightarrow \Lambda_Q \gamma$ have been investigated in [5] using the same framework. Some of these radiative transitions have also been previously studied using chiral perturbation theory [6], heavy quark and chiral symmetries [7, 8], relativistic quark model [9] and light cone QCD sum rules at leading order in HQET in [10].

The outline of the paper is as follows. In next section, QCD sum rules for the electromagnetic form factors of the transitions under consideration are calculated. In last section, we numerically analyze the obtained sum rules. This section also includes comparison of our

results with the predictions of VDM on the multipole moments as well as the corresponding decay widths.

2 Theoretical framework

The aim of this section is to obtain light cone QCD sum rules (LCQSR) for the electromagnetic form factors defining the radiative $\Omega_Q^* \rightarrow \Omega_Q \gamma$ and $\Xi_Q^* \rightarrow \Xi_Q \gamma$ transitions. For this goal we use the following two-point correlation function in the presence of an external photon field:

$$\Pi_\mu(p, q) = i \int d^4x e^{ip \cdot x} \langle 0 | T \{ \eta(x) \bar{\eta}_\mu(0) \} | 0 \rangle_\gamma, \quad (1)$$

where η and η_μ are the interpolating currents of the heavy flavored baryons with spin 1/2 and 3/2, respectively. The main task in the following is to calculate this correlation function once in terms of hadronic parameters called the hadronic side and in terms of photon distribution amplitudes (DAs) with increasing twist by the help of operator product expansion (OPE). By equating the coefficients of appropriate structures from hadronic to OPE side, we obtain LCQSR for the transition form factors. To suppress the contribution of the higher states and continuum, we apply Borel transformations with respect to the momentum squared of the initial and final baryonic states. For further pushing down those contributions, we also apply continuum subtraction to both sides of the LCQSRs obtained.

2.1 Hadronic side

To obtain the hadronic representation, we insert complete sets of intermediate states having the same quantum numbers as the interpolating currents into the above correlation function. As a result of which we get

$$\Pi_\mu(p, q) = \frac{\langle 0 | \eta | 2(p, s') \rangle \langle 2(p, s') | 1(p+q, s) \rangle_\gamma \langle 1(p+q, s) | \bar{\eta}_\mu | 0 \rangle}{p^2 - m_2^2} + \dots, \quad (2)$$

where the dots indicate the contributions of the higher states and continuum and q is the photon's momentum. In the above equation, $\langle 1(p+q, s) |$ and $\langle 2(p, s') |$ denote the heavy spin 3/2 and 1/2 states and m_1 and m_2 are their masses, respectively. To proceed, we need to know the matrix elements of the interpolating currents between the vacuum and the baryonic states. They are defined in terms of spinors and residues as

$$\begin{aligned} \langle 1(p+q, s) | \bar{\eta}_\mu(0) | 0 \rangle &= \lambda_1 \bar{u}_\mu(p+q, s), \\ \langle 0 | \eta(0) | 2(p, s') \rangle &= \lambda_2 u(p, s'), \end{aligned} \quad (3)$$

where $u_\mu(p, s)$ is the Rarita-Schwinger spinor; and λ_1 and λ_2 are the residues of the heavy baryons with spin 3/2 and 1/2, respectively which are calculated in [5]. The matrix element $\langle 2(p, s') | 1(p + q, s) \rangle_\gamma$ is also defined as [11, 12]

$$\begin{aligned} \langle 2(p, s') | 1(p + q, s) \rangle_\gamma &= e\bar{u}(p, s') \left\{ G_1(q_\mu \not{\epsilon} - \epsilon_\mu \not{q}) + G_2[(\mathcal{P}\epsilon)q_\mu - (\mathcal{P}q)\epsilon_\mu]\gamma_5 \right. \\ &\quad \left. + G_3[(q\epsilon)q_\mu - q^2\epsilon_\mu]\gamma_5 \right\} u_\mu(p + q, s), \end{aligned} \quad (4)$$

where G_i are electromagnetic form factors, ϵ_μ is the photon's polarization vector and $\mathcal{P} = \frac{p+(p+q)}{2}$. In the above equation, the term proportional to G_3 is zero for the real photon which we consider in the present study. At $q^2 = 0$, the transition magnetic dipole moment G_M and the electric quadrupole moment G_E are defined in terms of the remaining electromagnetic form factors as

$$\begin{aligned} G_M &= \left[(3m_1 + m_2)\frac{G_1}{m_1} + (m_1 - m_2)G_2 \right] \frac{m_2}{3}, \\ G_E &= (m_1 - m_2) \left[\frac{G_1}{m_1} + G_2 \right] \frac{m_2}{3}. \end{aligned} \quad (5)$$

Now, we use Eqs. (4) and (3) in Eq. (2) and perform summation over spins of the Dirac and Rarita-Schwinger spinors. In the case of spin 3/2 this summation is written as

$$\sum_s u_\mu(p, s)\bar{u}_\nu(p, s) = \frac{(\not{p} + m)}{2m} \left\{ -g_{\mu\nu} + \frac{1}{3}\gamma_\mu\gamma_\nu - \frac{2p_\mu p_\nu}{3m^2} - \frac{p_\mu\gamma_\nu - p_\nu\gamma_\mu}{3m} \right\}. \quad (6)$$

At this stage, we shall

- make all Lorentz structures independent of each other,
- eliminate the contributions of the spin 1/2 baryons which also couple to η_μ besides the spin 3/2 baryons.

To overcome those problems and separate the contributions of spin 3/2 baryons coupled to η_μ , we order the Dirac matrices in an appropriate way. In this work, we choose the ordering $\not{\epsilon} \not{q} \not{p} \gamma_\mu$ and get the following expression for the hadronic side of the correlation function:

$$\begin{aligned} \Pi_\mu &= e\lambda_1\lambda_2 \frac{1}{p^2 - m_2^2} \frac{1}{(p+q)^2 - m_1^2} \left[\right. \\ &\quad \left. \left[\epsilon_\mu(pq) - (\epsilon p)q_\mu \right] \left\{ -2G_1m_1 - G_2m_1m_2 + G_2(p+q)^2 \right\} \right. \end{aligned}$$

$$\begin{aligned}
& + \left[2G_1 - G_2(m_1 - m_2) \right] \not{p} + m_2 G_2 \not{q} - G_2 \not{q} \not{p} \Big\} \gamma_5 \\
& + \left[q_\mu \not{\epsilon} - \varepsilon_\mu \not{q} \right] \left\{ G_1(p^2 + m_1 m_2) - G_1(m_1 + m_2) \not{p} \right\} \gamma_5 \\
& + 2G_1 \left[\not{\epsilon}(pq) - \not{q}(\varepsilon p) \right] q_\mu \gamma_5 - G_1 \not{\epsilon} \not{q} (m_2 + \not{p}) q_\mu \gamma_5 \\
& + \text{other structures with } \gamma_\mu \text{ at the end or which are proportional to } (p + q)_\mu \Big], \tag{7}
\end{aligned}$$

where, we need two invariant structures to calculate the form factors G_1 and G_2 . In the present work, we select the structures $\not{\epsilon} \not{p} \gamma_5 q_\mu$ and $\not{q} \not{p} \gamma_5 (\varepsilon p) q_\mu$ for G_1 and G_2 , respectively. The advantage of these structures is that these terms do not receive contributions from contact terms.

2.2 OPE Side

On OPE side, the aforementioned correlation function is calculated in terms of QCD degrees of freedom and photon DAs. For this aim, we substitute the explicit forms of the interpolating currents of the heavy baryons into the correlation function in Eq. (1) and use the Wick's theorem to obtain the correlation in terms of quark propagators.

The interpolating currents for spin 3/2 baryons are taken as

$$\eta_\mu = A \epsilon^{abc} \left\{ (q_1^a C \gamma_\mu q_2^b) Q^c + (q_2^a C \gamma_\mu Q^b) q_1^c + (Q^a C \gamma_\mu q_1^b) q_2^c \right\}, \tag{8}$$

where q_1 and q_2 stand for light quarks; a , b and c are color indices and C is the charge conjugation operator. The normalization factor A and light quark content of heavy spin 3/2 baryons are presented in table 1:

| Heavy spin 3/2 baryons | A | q_1 | q_2 |
|-------------------------|--------------|-------|-------|
| $\Omega_{b(c)}^{*-(0)}$ | $1/\sqrt{3}$ | s | s |
| $\Xi_{b(c)}^{*0(+)}$ | $\sqrt{2/3}$ | s | u |
| $\Xi_{b(c)}^{*- (0)}$ | $\sqrt{2/3}$ | s | d |

Table 1: The normalization factor A and light quark content of heavy spin 3/2 baryons.

The general form of the interpolating currents for the heavy spin 1/2 baryons under consideration can be written as (see for instance [13])

$$\eta = -\frac{B}{\sqrt{2}} \epsilon^{abc} \left\{ (q_1^{aT} C Q^b) \gamma_5 q_2^c + \beta (q_1^{aT} C \gamma_5 Q^b) q_2^c - \left[(Q^{aT} C q_2^b) \gamma_5 q_1^c + \beta (Q^{aT} C \gamma_5 q_2^b) q_1^c \right] \right\},$$

(9)

where β is an arbitrary parameter and $\beta = -1$ corresponds to the Ioffe current. The constant B and quark fields q_1 and q_2 for the corresponding heavy spin 1/2 baryons are given in table 2.

| Heavy spin 3/2 baryons | B | q_1 | q_2 |
|----------------------------|--------------|-------|-------|
| $\Omega_{b(c)}^{-(0)}$ | $1/\sqrt{2}$ | s | s |
| $\Xi_{b(c)}^{\prime 0(+)}$ | 1 | s | u |
| $\Xi_{b(c)}^{\prime -(0)}$ | 1 | s | d |

Table 2: The constant B and light quark content of the heavy spin 1/2 baryons under consideration.

The correlation function in OPE side receives three different contributions: 1) perturbative contributions, 2) mixed contributions at which the photon is radiated from short distances and at least one of the quarks forms a condensate and 3) non-perturbative contributions where photon is radiated at long distances. The last contribution is parameterized by the matrix element $\langle \gamma(q) | \bar{q}(x_1)\Gamma q(x_2) | 0 \rangle$ which is expanded in terms of photon DAs with definite twists. Here Γ is the full set of Dirac matrices $\Gamma_j = \{1, \gamma_5, \gamma_\alpha, i\gamma_5\gamma_\alpha, \sigma_{\alpha\beta}/\sqrt{2}\}$.

The perturbative contribution at which the photon interacts with the quarks perturbatively, is obtained by replacing corresponding free quark propagator by

$$S_{\alpha\beta}^{ab} \Rightarrow \left\{ \int d^4y S^{free}(x-y) A S^{free}(y) \right\}_{\alpha\beta}^{ab}, \quad (10)$$

where the free light and heavy quark propagators are given as

$$\begin{aligned} S_q^{free} &= \frac{i \not{x}}{2\pi^2 x^4} - \frac{m_q}{4\pi^2 x^2}, \\ S_Q^{free} &= \frac{m_Q^2}{4\pi^2} \frac{K_1(m_Q \sqrt{-x^2})}{\sqrt{-x^2}} - i \frac{m_Q^2 \not{x}}{4\pi^2 x^2} K_2(m_Q \sqrt{-x^2}), \end{aligned} \quad (11)$$

with K_i being the Bessel functions.

The non-perturbative contributions are obtained by replacing one of the light quark propagators that emits a photon by

$$S_{\alpha\beta}^{ab} \rightarrow -\frac{1}{4} \bar{q}^a \Gamma_j q^b (\Gamma_j)_{\alpha\beta}, \quad (12)$$

where sum over j is applied, and the remaining by full quark propagators involving the perturbative as well as the non-perturbative parts. The full heavy and light quark propagators which we use in the present work are (see [14, 15])

$$\begin{aligned}
S_Q(x) &= S_Q^{free}(x) - ig_s \int \frac{d^4k}{(2\pi)^4} e^{-ikx} \int_0^1 dv \left[\frac{k + m_Q}{(m_Q^2 - k^2)^2} G^{\mu\nu}(vx) \sigma_{\mu\nu} \right. \\
&\quad \left. + \frac{1}{m_Q^2 - k^2} vx_\mu G^{\mu\nu} \gamma_\nu \right], \\
S_q(x) &= S_q^{free}(x) - \frac{m_q}{4\pi^2 x^2} - \frac{\langle \bar{q}q \rangle}{12} \left(1 - i \frac{m_q}{4} \not{x} \right) - \frac{x^2}{192} m_0^2 \langle \bar{q}q \rangle \left(1 - i \frac{m_q}{6} \not{x} \right) \\
&\quad - ig_s \int_0^1 du \left[\frac{\not{x}}{16\pi^2 x^2} G_{\mu\nu}(ux) \sigma_{\mu\nu} - ux^\mu G_{\mu\nu}(ux) \gamma^\nu \frac{i}{4\pi^2 x^2} \right. \\
&\quad \left. - i \frac{m_q}{32\pi^2} G_{\mu\nu} \sigma^{\mu\nu} \left(\ln \left(\frac{-x^2 \Lambda^2}{4} \right) + 2\gamma_E \right) \right], \tag{13}
\end{aligned}$$

where Λ is the scale parameter and we choose it at factorization scale $\Lambda = (0.5 - 1) \text{ GeV}$ [16].

In order to calculate the non-perturbative contributions, we need the matrix elements $\langle \gamma(q) | \bar{q} \Gamma_i q | 0 \rangle$. These matrix elements are determined in terms of the photon DAs as [17]

$$\begin{aligned}
\langle \gamma(q) | \bar{q}(x) \sigma_{\mu\nu} q(0) | 0 \rangle &= -ie_q \bar{q}q (\varepsilon_\mu q_\nu - \varepsilon_\nu q_\mu) \int_0^1 du e^{i\bar{u}qx} \left(\chi \varphi_\gamma(u) + \frac{x^2}{16} \mathbb{A}(u) \right) \\
&\quad - \frac{i}{2(qx)} e_q \langle \bar{q}q \rangle \left[x_\nu \left(\varepsilon_\mu - q_\mu \frac{\varepsilon x}{qx} \right) - x_\mu \left(\varepsilon_\nu - q_\nu \frac{\varepsilon x}{qx} \right) \right] \int_0^1 du e^{i\bar{u}qx} h_\gamma(u), \\
\langle \gamma(q) | \bar{q}(x) \gamma_\mu q(0) | 0 \rangle &= e_q f_{3\gamma} \left(\varepsilon_\mu - q_\mu \frac{\varepsilon x}{qx} \right) \int_0^1 du e^{i\bar{u}qx} \psi^v(u), \\
\langle \gamma(q) | \bar{q}(x) \gamma_\mu \gamma_5 q(0) | 0 \rangle &= -\frac{1}{4} e_q f_{3\gamma} \varepsilon_{\mu\nu\alpha\beta} \varepsilon^\nu q^\alpha x^\beta \int_0^1 du e^{i\bar{u}qx} \psi^a(u), \\
\langle \gamma(q) | \bar{q}(x) g_s G_{\mu\nu}(vx) q(0) | 0 \rangle &= -ie_q \langle \bar{q}q \rangle (\varepsilon_\mu q_\nu - \varepsilon_\nu q_\mu) \int \mathcal{D}\alpha_i e^{i(\alpha_{\bar{q}} + v\alpha_g)qx} \mathcal{S}(\alpha_i), \\
\langle \gamma(q) | \bar{q}(x) g_s \tilde{G}_{\mu\nu} i\gamma_5(vx) q(0) | 0 \rangle &= -ie_q \langle \bar{q}q \rangle (\varepsilon_\mu q_\nu - \varepsilon_\nu q_\mu) \int \mathcal{D}\alpha_i e^{i(\alpha_{\bar{q}} + v\alpha_g)qx} \tilde{\mathcal{S}}(\alpha_i), \\
\langle \gamma(q) | \bar{q}(x) g_s \tilde{G}_{\mu\nu}(vx) \gamma_\alpha \gamma_5 q(0) | 0 \rangle &= e_q f_{3\gamma} q_\alpha (\varepsilon_\mu q_\nu - \varepsilon_\nu q_\mu) \int \mathcal{D}\alpha_i e^{i(\alpha_{\bar{q}} + v\alpha_g)qx} \mathcal{A}(\alpha_i), \\
\langle \gamma(q) | \bar{q}(x) g_s G_{\mu\nu}(vx) i\gamma_\alpha q(0) | 0 \rangle &= e_q f_{3\gamma} q_\alpha (\varepsilon_\mu q_\nu - \varepsilon_\nu q_\mu) \int \mathcal{D}\alpha_i e^{i(\alpha_{\bar{q}} + v\alpha_g)qx} \mathcal{V}(\alpha_i), \\
\langle \gamma(q) | \bar{q}(x) \sigma_{\alpha\beta} g_s G_{\mu\nu}(vx) q(0) | 0 \rangle &= e_q \langle \bar{q}q \rangle \left\{ \left[\left(\varepsilon_\mu - q_\mu \frac{\varepsilon x}{qx} \right) \left(g_{\alpha\nu} - \frac{1}{qx} (q_\alpha x_\nu + q_\nu x_\alpha) \right) q_\beta \right. \right. \\
&\quad - \left. \left(\varepsilon_\mu - q_\mu \frac{\varepsilon x}{qx} \right) \left(g_{\beta\nu} - \frac{1}{qx} (q_\beta x_\nu + q_\nu x_\beta) \right) q_\alpha \right. \\
&\quad \left. - \left(\varepsilon_\nu - q_\nu \frac{\varepsilon x}{qx} \right) \left(g_{\alpha\mu} - \frac{1}{qx} (q_\alpha x_\mu + q_\mu x_\alpha) \right) q_\beta \right. \\
&\quad \left. - \left(\varepsilon_\nu - q_\nu \frac{\varepsilon x}{qx} \right) \left(g_{\beta\mu} - \frac{1}{qx} (q_\beta x_\mu + q_\mu x_\beta) \right) q_\alpha \right\}
\end{aligned}$$

$$\begin{aligned}
& + \left(\varepsilon_\nu - q_\nu \frac{\varepsilon x}{q \cdot x} \right) \left(g_{\beta\mu} - \frac{1}{qx} (q_\beta x_\mu + q_\mu x_\beta) \right) q_\alpha \Big] \int \mathcal{D}\alpha_i e^{i(\alpha_{\bar{q}} + \nu\alpha_g)qx} \mathcal{T}_1(\alpha_i) \\
& + \left[\left(\varepsilon_\alpha - q_\alpha \frac{\varepsilon x}{q \cdot x} \right) \left(g_{\mu\beta} - \frac{1}{qx} (q_\mu x_\beta + q_\beta x_\mu) \right) q_\nu \right. \\
& - \left(\varepsilon_\alpha - q_\alpha \frac{\varepsilon x}{q \cdot x} \right) \left(g_{\nu\beta} - \frac{1}{qx} (q_\nu x_\beta + q_\beta x_\nu) \right) q_\mu \\
& - \left(\varepsilon_\beta - q_\beta \frac{\varepsilon x}{q \cdot x} \right) \left(g_{\mu\alpha} - \frac{1}{qx} (q_\mu x_\alpha + q_\alpha x_\mu) \right) q_\nu \\
& \left. + \left(\varepsilon_\beta - q_\beta \frac{\varepsilon x}{q \cdot x} \right) \left(g_{\nu\alpha} - \frac{1}{qx} (q_\nu x_\alpha + q_\alpha x_\nu) \right) q_\mu \right] \int \mathcal{D}\alpha_i e^{i(\alpha_{\bar{q}} + \nu\alpha_g)qx} \mathcal{T}_2(\alpha_i) \\
& + \frac{1}{qx} (q_\mu x_\nu - q_\nu x_\mu) (\varepsilon_\alpha q_\beta - \varepsilon_\beta q_\alpha) \int \mathcal{D}\alpha_i e^{i(\alpha_{\bar{q}} + \nu\alpha_g)qx} \mathcal{T}_3(\alpha_i) \\
& + \frac{1}{qx} (q_\alpha x_\beta - q_\beta x_\alpha) (\varepsilon_\mu q_\nu - \varepsilon_\nu q_\mu) \int \mathcal{D}\alpha_i e^{i(\alpha_{\bar{q}} + \nu\alpha_g)qx} \mathcal{T}_4(\alpha_i) \Big\}, \tag{14}
\end{aligned}$$

where $\varphi_\gamma(u)$ is the leading twist 2, $\psi^v(u)$, $\psi^a(u)$, \mathcal{A} and \mathcal{V} are the twist 3; and $h_\gamma(u)$, \mathbb{A} and \mathcal{T}_i ($i = 1, 2, 3, 4$) are the twist 4 photon DAs [17]. Here χ is the magnetic susceptibility of the quarks.

The measure $\int \mathcal{D}\alpha_i$ is defined as

$$\int \mathcal{D}\alpha_i = \int_0^1 d\alpha_{\bar{q}} \int_0^1 d\alpha_q \int_0^1 d\alpha_g \delta(1 - \alpha_{\bar{q}} - \alpha_q - \alpha_g). \tag{15}$$

In order to obtain the sum rules for the form factors G_1 and G_2 , we equate the coefficients of the structures $\not{\epsilon} \not{p} \gamma_5 q_\mu$ and $\not{\not{A}} \not{p} \gamma_5 (\varepsilon p) q_\mu$ from both hadronic and OPE representations of the same correlation function. We apply the Borel transformations with respect to the variables p^2 and $(p+q)^2$ as well as continuum subtraction to suppress the contributions of the higher states and continuum. Finally, we obtain the following schematically written sum rules for the electromagnetic form factors G_1 and G_2 :

$$\begin{aligned}
G_1 &= -\frac{1}{\lambda_1 \lambda_2 (m_1 + m_2)} e^{\frac{m_1^2}{M_1^2}} e^{\frac{m_2^2}{M_2^2}} \left[e_{q_1} \Pi_1 + e_{q_2} \Pi_1(q_1 \leftrightarrow q_2) + e_Q \Pi'_1 \right] \\
G_2 &= \frac{1}{\lambda_1 \lambda_2} e^{\frac{m_1^2}{M_1^2}} e^{\frac{m_2^2}{M_2^2}} \left[e_{q_1} \Pi_2 + e_{q_2} \Pi_2(q_1 \leftrightarrow q_2) + e_Q \Pi'_2 \right], \tag{16}
\end{aligned}$$

where the functions $\Pi_i[\Pi'_i]$ can be written as

$$\Pi_i[\Pi'_i] = \int_{m_Q^2}^{s_0} e^{\frac{-s}{M^2}} \rho_i(s) [\rho'_i(s)] ds + e^{\frac{-m_Q^2}{M^2}} \Gamma_i[\Gamma'_i], \tag{17}$$

where s_0 is the continuum threshold and we take $M_1^2 = M_2^2 = 2M^2$ since the masses of the initial and final baryons are close to each other. The spectral densities $\rho_i(s) [\rho'_i(s)]$ and the functions $\Gamma_i[\Gamma'_i]$ are very lengthy, hence, we do not present their explicit expressions here.

3 Numerical results

In this part, we numerically analyze the sum rules for the magnetic dipole G_M and electric quadrupole G_E obtained in the previous section. For this aim, we use the input parameters $\langle \bar{u}u \rangle(1 \text{ GeV}) = \langle \bar{d}d \rangle(1 \text{ GeV}) = -(0.243)^3 \text{ GeV}^3$, $\beta(1 \text{ GeV}) = 0.8\langle \bar{u}u \rangle(1 \text{ GeV})$, $m_0^2(1 \text{ GeV}) = (0.8 \pm 0.2) \text{ GeV}^2$ [18] and $f_{3\gamma} = -0.0039 \text{ GeV}^2$ [17]. The value of the magnetic susceptibility are calculated in [19, 20, 21]. Here we use the value $\chi(1 \text{ GeV}) = -4.4 \text{ GeV}^{-2}$ [21] for this quantity. The LCQSR for the magnetic dipole and electric quadrupole moments also include the photon DAs [17] whose expressions are given as

$$\begin{aligned}
\varphi_\gamma(u) &= 6u\bar{u} \left(1 + \varphi_2(\mu) C_2^{\frac{3}{2}}(u - \bar{u}) \right), \\
\psi^v(u) &= 3 \left(3(2u - 1)^2 - 1 \right) + \frac{3}{64} (15w_\gamma^V - 5w_\gamma^A) \left(3 - 30(2u - 1)^2 + 35(2u - 1)^4 \right), \\
\psi^a(u) &= \left(1 - (2u - 1)^2 \right) \left(5(2u - 1)^2 - 1 \right) \frac{5}{2} \left(1 + \frac{9}{16}w_\gamma^V - \frac{3}{16}w_\gamma^A \right), \\
\mathcal{A}(\alpha_i) &= 360\alpha_q\alpha_{\bar{q}}\alpha_g^2 \left(1 + w_\gamma^A \frac{1}{2}(7\alpha_g - 3) \right), \\
\mathcal{V}(\alpha_i) &= 540w_\gamma^V(\alpha_q - \alpha_{\bar{q}})\alpha_q\alpha_{\bar{q}}\alpha_g^2, \\
h_\gamma(u) &= -10 \left(1 + 2\kappa^+ \right) C_2^{\frac{1}{2}}(u - \bar{u}), \\
\mathbb{A}(u) &= 40u^2\bar{u}^2 \left(3\kappa - \kappa^+ + 1 \right) \\
&\quad + 8(\zeta_2^+ - 3\zeta_2) [u\bar{u}(2 + 13u\bar{u}) \\
&\quad + 2u^3(10 - 15u + 6u^2) \ln(u) + 2\bar{u}^3(10 - 15\bar{u} + 6\bar{u}^2) \ln(\bar{u})], \\
\mathcal{T}_1(\alpha_i) &= -120(3\zeta_2 + \zeta_2^+)(\alpha_{\bar{q}} - \alpha_q)\alpha_{\bar{q}}\alpha_q\alpha_g, \\
\mathcal{T}_2(\alpha_i) &= 30\alpha_g^2(\alpha_{\bar{q}} - \alpha_q) \left((\kappa - \kappa^+) + (\zeta_1 - \zeta_1^+)(1 - 2\alpha_g) + \zeta_2(3 - 4\alpha_g) \right), \\
\mathcal{T}_3(\alpha_i) &= -120(3\zeta_2 - \zeta_2^+)(\alpha_{\bar{q}} - \alpha_q)\alpha_{\bar{q}}\alpha_q\alpha_g, \\
\mathcal{T}_4(\alpha_i) &= 30\alpha_g^2(\alpha_{\bar{q}} - \alpha_q) \left((\kappa + \kappa^+) + (\zeta_1 + \zeta_1^+)(1 - 2\alpha_g) + \zeta_2(3 - 4\alpha_g) \right), \\
\mathcal{S}(\alpha_i) &= 30\alpha_g^2 \{ (\kappa + \kappa^+)(1 - \alpha_g) + (\zeta_1 + \zeta_1^+)(1 - \alpha_g)(1 - 2\alpha_g) \\
&\quad + \zeta_2[3(\alpha_{\bar{q}} - \alpha_q)^2 - \alpha_g(1 - \alpha_g)] \}, \\
\tilde{\mathcal{S}}(\alpha_i) &= -30\alpha_g^2 \{ (\kappa - \kappa^+)(1 - \alpha_g) + (\zeta_1 - \zeta_1^+)(1 - \alpha_g)(1 - 2\alpha_g) \\
&\quad + \zeta_2[3(\alpha_{\bar{q}} - \alpha_q)^2 - \alpha_g(1 - \alpha_g)] \}, \tag{18}
\end{aligned}$$

where, the constants inside the DAs are given by $\varphi_2(1 \text{ GeV}) = 0$, $w_\gamma^V = 3.8 \pm 1.8$, $w_\gamma^A = -2.1 \pm 1.0$, $\kappa = 0.2$, $\kappa^+ = 0$, $\zeta_1 = 0.4$, $\zeta_2 = 0.3$, $\zeta_1^+ = 0$ and $\zeta_2^+ = 0$ [17].

The sum rules for the electromagnetic form factors contain three more auxiliary param-

eters: Borel mass parameter M^2 , the continuum threshold s_0 and the arbitrary parameter β entering the expressions of the interpolating currents of the heavy spin 1/2 baryons. Any physical quantities, like the magnetic dipole and electric quadrupole moments, should be independent of these auxiliary parameters. Therefore, we try to find “working regions” for these auxiliary parameters such that in these regions the G_M and G_E are practically independent of these parameters. The upper and lower bands for M^2 are found requiring that not only the contributions of the higher states and continuum are less than the ground state contribution, but also the contributions of the higher twists are less compared to the leading twists. By these requirements, the working regions of Borel mass parameter are obtained as $15 \text{ GeV}^2 \leq M^2 \leq 30 \text{ GeV}^2$ and $6 \text{ GeV}^2 \leq M^2 \leq 12 \text{ GeV}^2$ for baryons containing b and c quarks, respectively. The continuum threshold s_0 depends on the energy of the first excited state of the initial channel and is found for different channels as $6.3^2[6.4^2] \text{ (GeV}^2) \leq s_0 \leq 6.5^2[6.6^2] \text{ GeV}^2$ for the $\Xi_b^*[\Omega_b^*] \rightarrow \Xi_b'[\Omega_b']\gamma$ and $2.7^2[2.9^2] \text{ (GeV}^2) \leq s_0 \leq 2.9^2[3.1^2] \text{ GeV}^2$ for the $\Xi_c^*[\Omega_c^*] \rightarrow \Xi_c'[\Omega_c']\gamma$ transitions. The dependence of the magnetic dipole moment G_M and electric quadrupole moment G_E on the Borel mass parameter at different fixed values of the continuum threshold and general parameter β are depicted in figures 1-6 for the radiative transitions under consideration.

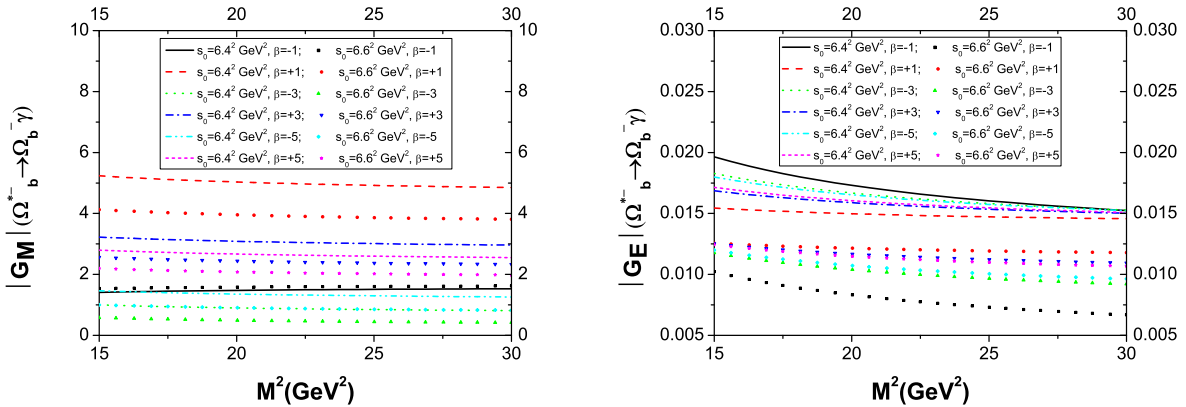


Figure 1: **Left:** The dependence of the magnetic dipole moment G_M for $\Omega_b^{*-} \rightarrow \Omega_b^- \gamma$ transition on the Borel mass parameter M^2 . **Right:** The dependence of the electric quadrupole moment G_E for $\Omega_b^{*-} \rightarrow \Omega_b^- \gamma$ transition on the Borel mass parameter M^2 .

Note that, in all figures, we plot the absolute values of the physical quantities under study since it is not possible to predict the signs of the residues from the mass sum rules. From these figures, we see that the results weakly depend on the M^2 and s_0 in their working regions.

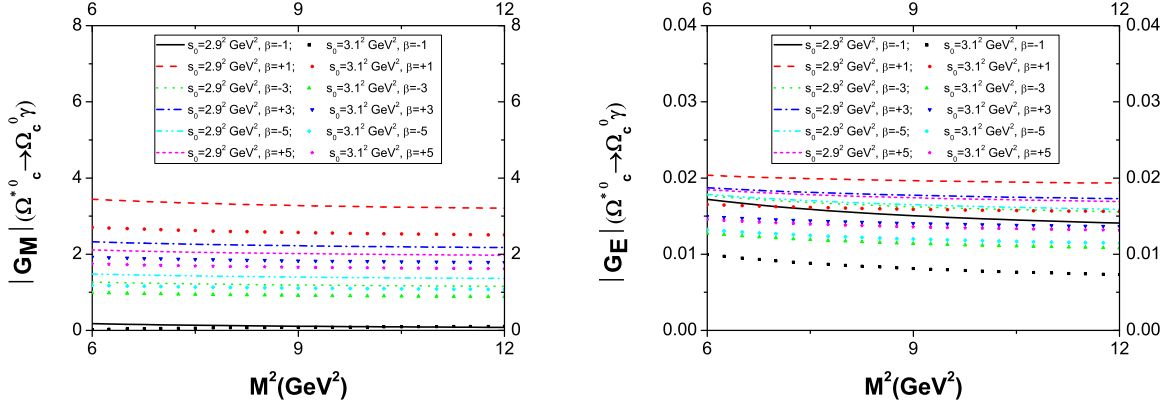


Figure 2: The same as Fig. 1, but for $\Omega_c^{*0} \rightarrow \Omega_c^0 \gamma$.

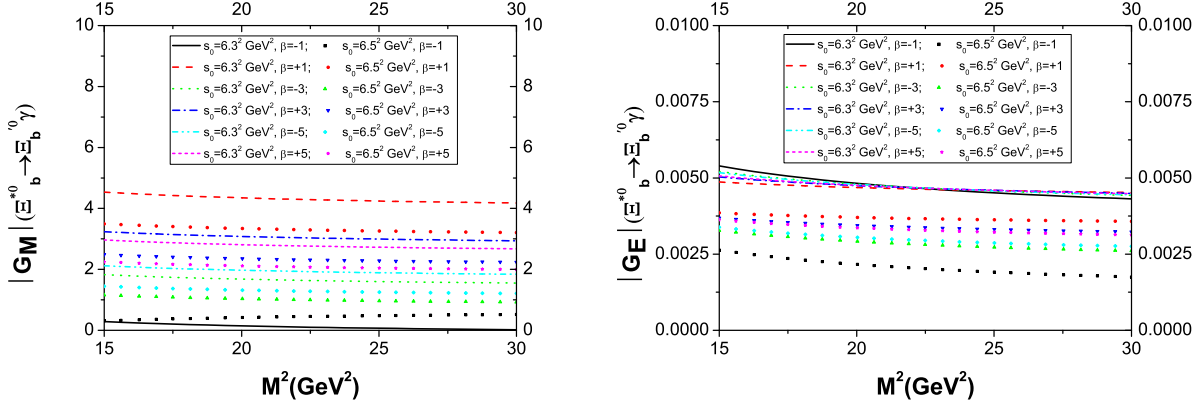


Figure 3: The same as Fig. 1, but for $\Xi_b^{*0} \rightarrow \Xi_b^0 \gamma$.

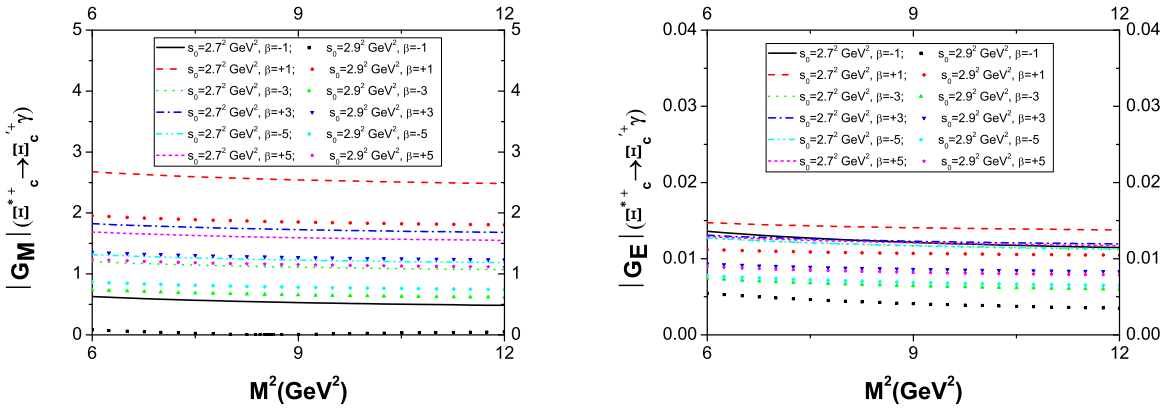


Figure 4: The same as Fig. 1, but for $\Xi_c^{*+} \rightarrow \Xi_c^+ \gamma$.

To determine the working regions for the general parameter β at different radiative channels, we depict the dependence of the results on this parameter at different fixed values

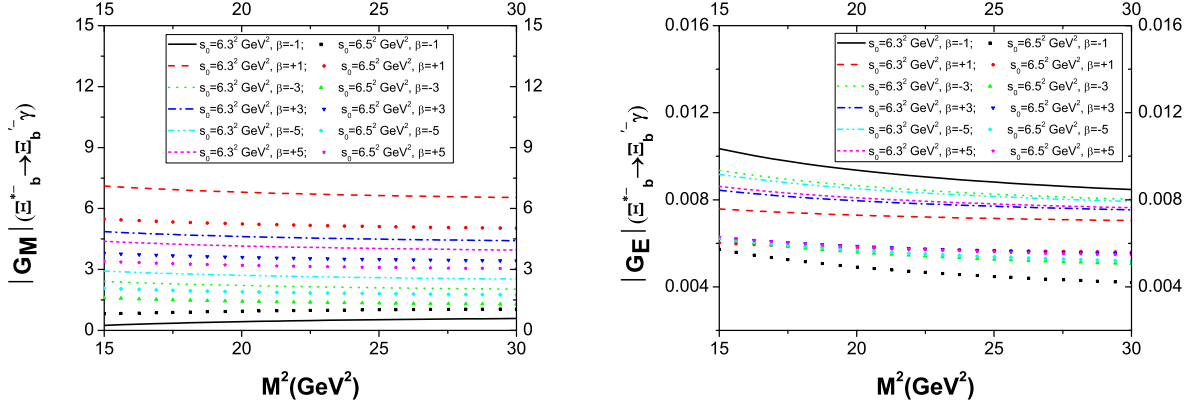


Figure 5: The same as Fig. 1, but for $\Xi_b^{*-} \rightarrow \Xi_b'^- \gamma$.

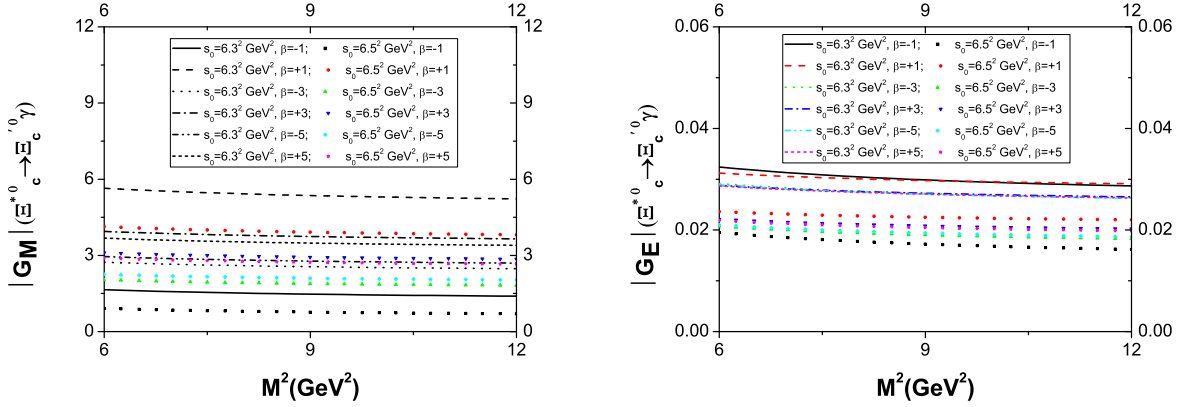


Figure 6: The same as Fig. 1, but for $\Xi_c^{*0} \rightarrow \Xi_c'^0 \gamma$.

of the Borel mass parameter and continuum threshold in figures 7-12. Note that instead of β we use $\cos\theta$, where $\beta = \tan\theta$. The interval $-1 \leq \cos\theta \leq 1$ corresponds to β between $-\infty$ to $+\infty$ which we shall consider in our calculations. The numerical results show that the values of G_E are negligibly small and therefore we consider only dependence of G_M on β , in order to find its working region.

From figures 7-12, we obtain the region $-0.25 \leq \cos\theta \leq 0.5$ common for all radiative transitions under consideration, at which the dependence of the G_M on $\cos\theta$ is relatively weak. In most of the figures related to the magnetic dipole moment, the Ioffe current which corresponds to $\cos\theta \simeq -0.71$ remains out of the reliable region.

Considering the working regions for the auxiliary parameters, photon DAs and other input parameters, we extract the values of the magnetic dipole moment G_M and the electric quadrupole moment G_E correspond to the considered radiative transitions as presented in

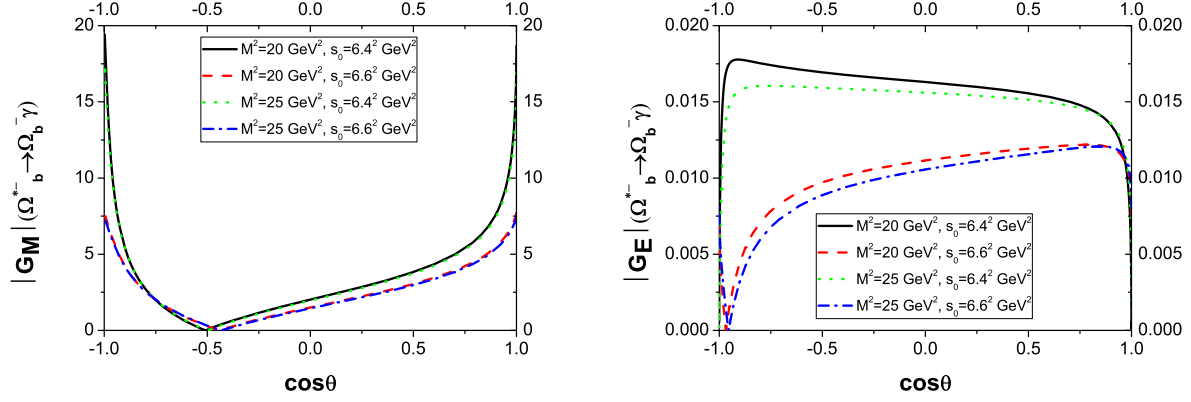


Figure 7: **Left:** The dependence of the magnetic dipole moment G_M for $\Omega_b^{*-} \rightarrow \Omega_b^- \gamma$ on $\cos\theta$. **Right:** The dependence of the electric quadrupole moment G_E for $\Omega_b^{*-} \rightarrow \Omega_b^- \gamma$ on $\cos\theta$.

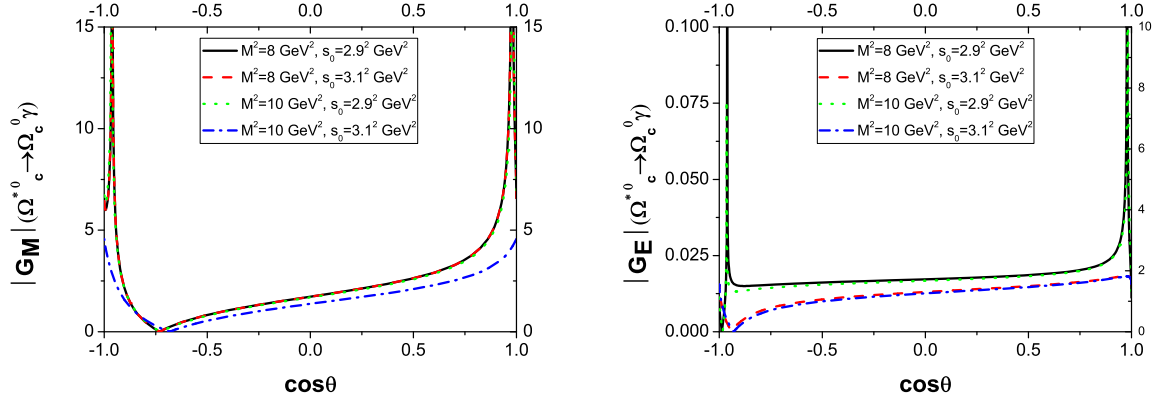


Figure 8: The same as Fig. 7, but for $\Omega_c^{*0} \rightarrow \Omega_c^0 \gamma$.

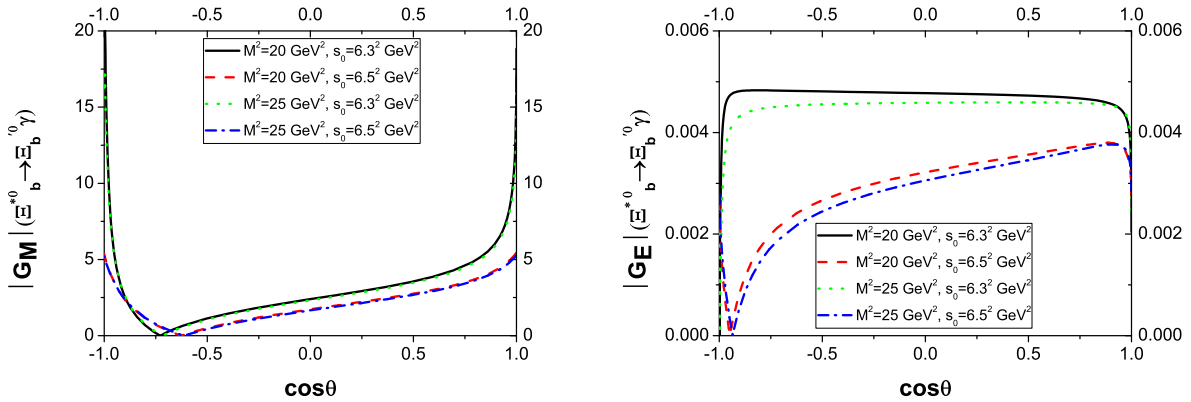


Figure 9: The same as Fig. 7, but for $\Xi_b^{*0} \rightarrow \Xi_b^0 \gamma$.

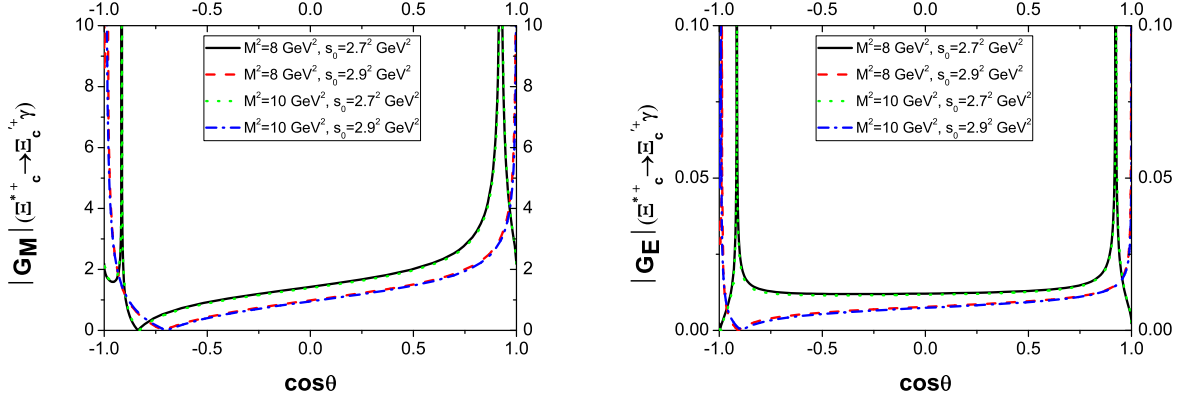


Figure 10: The same as Fig. 7, but for $\Xi_c^{*+} \rightarrow \Xi_c^+ \gamma$.

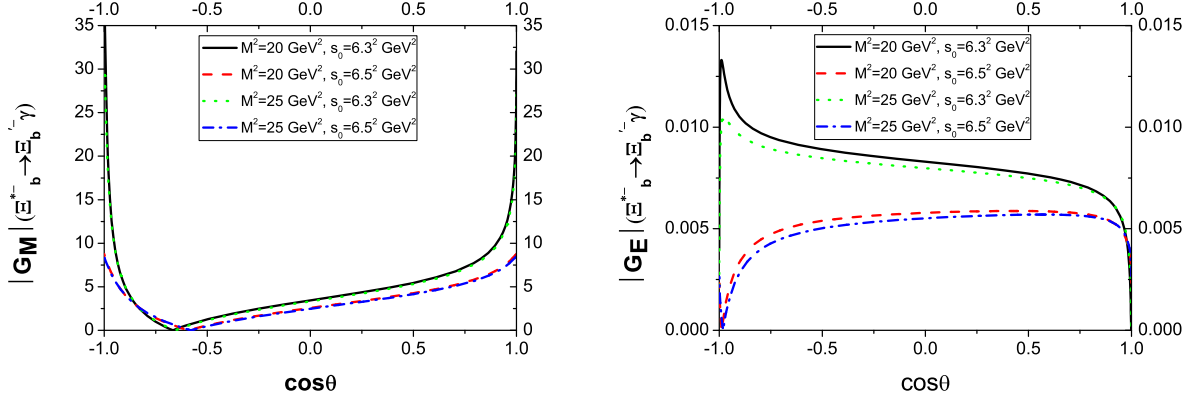


Figure 11: The same as Fig. 7, but for $\Xi_b^{*-} \rightarrow \Xi_b^- \gamma$.

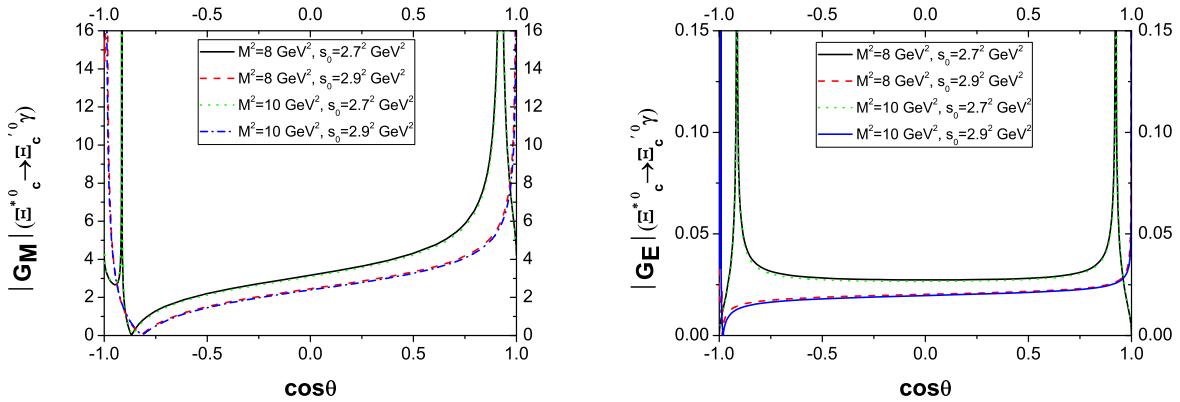


Figure 12: The same as Fig. 7, but for $\Xi_c^{*0} \rightarrow \Xi_c^0 \gamma$.

table 3. For comparison, we also present the predictions of VDM [3] on G_M and G_E in this table. From this table we see that, within the errors, our predictions are comparable

with those of VDM on the magnetic dipole moment G_M for all transitions except that $\Omega_b^{*-} \rightarrow \Omega_b^- \gamma$ which our result is considerably small compared to that of VDM. In both models, the values of G_E are negligibly small for all considered channels.

| | $ G_M $ (PW) | $ G_E $ (PW) | $ G_M $ (VDM) [3] | $ G_E $ (VDM) [3] |
|---|-------------------|--------------|-------------------|-------------------|
| $\Omega_b^{*-} \rightarrow \Omega_b^- \gamma$ | 2.724 ± 0.807 | 0.013 | 4.52 | 0.034 |
| $\Omega_c^{*0} \rightarrow \Omega_c^0 \gamma$ | 2.134 ± 0.712 | 0.016 | 2.17 | 0.026 |
| $\Xi_b^{*0} \rightarrow \Xi_b^0 \gamma$ | 2.828 ± 0.808 | 0.004 | 2.93 | 0.017 |
| $\Xi_c^{*+} \rightarrow \Xi_c^+ \gamma$ | 1.583 ± 0.495 | 0.011 | 1.33 | 0.019 |
| $\Xi_b^{*-} \rightarrow \Xi_b'^- \gamma$ | 4.048 ± 1.418 | 0.007 | 4.63 | 0.021 |
| $\Xi_c^{*0} \rightarrow \Xi_c'^0 \gamma$ | 2.802 ± 0.902 | 0.024 | 2.20 | 0.026 |

Table 3: The absolute values of the magnetic dipole moment $|G_M|$ and electric quadrupole moment $|G_E|$ for the corresponding radiative decays in units of natural magneton. PW means present work and VDM refers to the vector dominance model.

At the end of this section we would like to present the decay width for the radiative transitions under consideration. Considering the transition matrix element in Eq. (4) and definitions of the magnetic dipole and electric quadrupole moments in terms of form factors G_1 and G_2 , we get the following formula for the widths of the corresponding transitions:

$$\Gamma = 3 \frac{\alpha}{32} \frac{(m_1^2 - m_2^2)^3}{m_1^3 m_2^2} (G_M^2 + 3G_E^2). \quad (19)$$

Using the numerical values for the magnetic dipole and electric quadrupole moments, we get the values for the widths as presented in table 4. For comparison, we also depict the existing predictions from the VDM in the same table. Looking at this table we see that our results are overall very close to the results of [3]. When we compare our results with those of [22, 23], we see considerable differences in orders of magnitudes between predictions of these two works except for $\Omega_c^{*0} \rightarrow \Omega_c^0 \gamma$ and $\Xi_c^{*+} \rightarrow \Xi_c^+ \gamma$ channels. The big differences between our result and [3] with those of [22, 23] can be attributed to the different baryon masses that are used since the width in Eq. (19) is very sensitive to the masses of the initial and final baryons.

In summary, we calculated the transition magnetic dipole moment G_M and electric quadrupole moment G_E as well as decay width for the radiative $\Omega_Q^* \rightarrow \Omega_Q \gamma$ and $\Xi_Q^* \rightarrow \Xi_Q' \gamma$ transitions within the light cone QCD sum rule approach and compared the results with the predictions of the VDM. Considering the recent progresses on the identification and

| | Γ (PW) | Γ (VDM) [3] | Γ (VDM) [22, 23] |
|---|---------------|--------------------|-------------------------|
| $\Omega_b^{*-} \rightarrow \Omega_b^- \gamma$ | 1.043 | 2.873 | 0.00074 |
| $\Omega_c^{*0} \rightarrow \Omega_c^0 \gamma$ | 1.391 | 1.439 | 1.16 |
| $\Xi_b^{*0} \rightarrow \Xi_b'^0 \gamma$ | 0.262 | 0.281 | 0.047 |
| $\Xi_c^{*+} \rightarrow \Xi_c'^+ \gamma$ | 0.681 | 0.485 | 0.96 |
| $\Xi_b^{*-} \rightarrow \Xi_b'^- \gamma$ | 0.538 | 0.702 | 0.066 |
| $\Xi_c^{*0} \rightarrow \Xi_c'^0 \gamma$ | 2.136 | 1.317 | 0.12 |

Table 4: Widths of the corresponding radiative transitions in KeV.

spectroscopy of the heavy baryons, we hope it will be possible to study these radiative decay channels at the experiment in near future.

4 Acknowledgment

K. A. and H. S. would like to thank TUBITAK for their partial financial support through the project 114F018.

References

- [1] M. Mattson et.al, SELEX Collaboration, Phys. Rev. Lett. 89, 112001 (2002).
- [2] A. Ocherashvili et.al, SELEX Collaboration, Phys. Lett. B 628, 18 (2005).
- [3] T. M. Aliev, M. Savci, V. S. Zamiralov, Mod. Phys. Lett. A 27, 1250054 (2012).
- [4] T. M. Aliev, K. Azizi, M. Savci, V. S. Zamiralov, Phys. Rev.D 83, 006007 (2011).
- [5] T. M. Aliev, K. Azizi, A. Ozpineci, Phys. Rev.D 79, 056005 (2009).
- [6] M. Banuls, A. Pich, I. Scimemi, Phys. Rev. D 61, 094009 (2000).
- [7] H. Y. Cheng, et. al, Phys. Rev. D 47, 1030 (1993).
- [8] S. Tawfig, J. G. Koerner, P. J.O'Donnel, Phys. Rev. D 63, 034005 (2001).
- [9] M. A. Ivanov, et. al, Phys. Rev. D 60, 094002 (1999).
- [10] S. L. Zhu, Y. B. Dai, Phys. Rev. D 59, 114015 (1999).

- [11] H. F. Joens, M. D. Scadron, *Ann. Phys.* 81, 1 (1973).
- [12] R. C. E. Devenish, T.S. Eisenschitz and J. G. Korner, *Phys. Rev. D* 14, 3063 (1976).
- [13] E. Bagan, M. Chabab, H. G. Dosch and S. Narison, *Phys. Lett. B* 278, 369 (1992).
- [14] I. I. Balitsky, V. M. Braun, *Nucl. Phys. B* 311, 541 (1989).
- [15] V. M. Braun, I. E. Filyanov, *Z. Phys. C* 48, 239 (1990).
- [16] K. G. Chetyrkin, A. Khodjamirian, A. A. Pivovarov, *Phys. Lett. B* 661, 250 (2008); I. I. Balitsky, V. M. Braun, A. V. Kolesnichenko, *Nucl. Phys. B* 312, 509 (1989).
- [17] P. Ball, V. M. Braun, N. Kivel, *Nucl. Phys. B* 649, 263 (2003).
- [18] V. M. Belyaev, B. L. Ioffe, *JETP* 56, 493 (1982).
- [19] J. Rohrwild, *JHEP* 0709, 073 (2007).
- [20] I. I. Balitsky, A. V. Kolesnichenko, A. V. Yung, *Yad. Fiz.* 41, 282 (1985).
- [21] V. M. Belyaev, I. I. Kogan, *Yad. Fiz.* 40, 1035 (1984).
- [22] Zhi-Gang Wang, *Eur. Phys. J. A*, 44, 105 (2010).
- [23] Zhi-Gang Wang, *Phys. Rev. D*, 81, 036002 (2010).